JFE TECHNICAL REPORT
No. 20 (Mar. 2015)

Effect of Microstructure on Fatigue Crack Growth Rate†

IGI Satoshi[*1] SADASUE Teruki[*2] OHMORI Akio[*3]

Abstract:

Recently various trials to reduce life cycle cost (LCC) by the improvement of fatigue life of welded steel structures were performed actively by heavy industrial fabricators. JFE Steel has developed the excellent fatigue resistant steel plate "AFD™" which reduces the fatigue growth rate with a half level to that of conventional steels. In the AFD™, uniformly and finely dispersed perlite in ferrite matrix contributed to achieve good fatigue properties, however the detailed mechanism has not been fully understood yet. In this paper, investigation results on the relationship between fatigue growth rate and perlite morphologies using fatigue testing equipment in the scanning electron microscope (SEM) which enables in-situ observation is introduced.

1. Introduction

One of the major concerns in maintaining the integrity of ship, bridges, and other large-scale structures is fatigue damage caused by cyclic stress in service[1)]. In welded structures, fatigue cracks firstly initiate from the weld toe as a result of large stress concentration, and in some cases those cracks grow until ultimate penetration and failure occur. It has been reported, for example, that reduction of stress concentration by TIG dressing or grinder treatment, or eliminating tensile residual stress and imparting compressive residual stress by hammer peening are effective for preventing initiation of fatigue cracks in welded joints[2,3)]. Realistically, however, it would be difficult to apply this kind of treatment to all the welds in an actual steel structure. Therefore, a technique in which the steel plate itself prevents growth of fatigue cracks is considered effective for extending the total fatigue life of steel structures.

Conventionally, the fatigue crack growth rate of steel materials was thought to show little sensitivity to the microstructure and mechanical properties of the steel[4)]. In contrast to this, focusing on the pearlite morphology, JFE Steel developed a high fatigue resistance steel plate, AFD™ (Anti-Fatigue Damage steel plate), in which fatigue properties are improved by uniformly and finely dispersing pearlite in the ferrite matrix by applying thermo-mechanical control process (TMCP) and the JFE Steel's on-line accelerated cooling device *Super*-OLAC™. [5)] In the second stage, in which a fatigue crack grows continuously and the growth rate da/dN is considered to follow Paris' Law, namely, $da/dN=C(\Delta K)^m$, AFD™ reduces the fatigue crack growth rate to 1/2 of the upper bound of the data band of the conventional

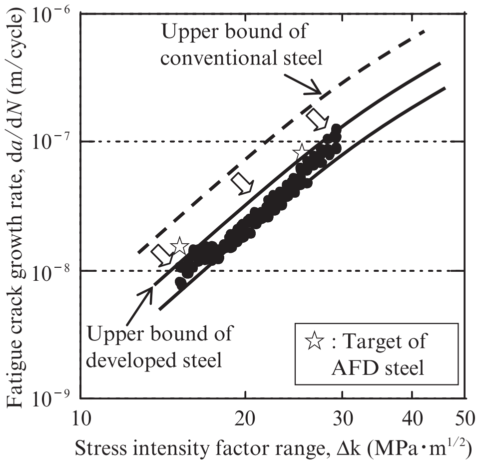

Fig. 1 Fatigue crack growth rate of AFD™ steel

† Originally published in *JFE GIHO* No. 33 (Feb. 2014), p. 55–61


*1 Dr. Eng.,
Senior Researcher Deputy General Manager,
Joining & Strength Res. Dept.,
Steel Res. Lab.,
JFE Steel


*2 Dr. Eng.,
Senior Researcher Deputy Manager,
Joining & Strength Res. Dept.,
Steel Res. Lab.,
JFE Steel


*3 Dr. Eng.,
Senior Researcher Manager,
Steel Products Res. Dept.,
Steel Res. Lab.,
JFE Steel

steel (**Fig. 1**). However, the detailed mechanism of this decrease in the fatigue crack growth rate had not necessarily been clarified. In particular, there was little knowledge of the relationship between the microscopic pearlite morphology, the crack propagation path, and crack closure behavior.

In this paper, the fatigue crack propagation behavior of two types of ferrite-pearlite dual-phase steels were studied by using a fatigue crack propagation test in a scanning electron microscope barrel and an in-*situ* observation technique. In particular, the effect of the pearlite morphology on fatigue crack growth resistance under the condition of a constant ΔK in the second stage was studied in detail from the viewpoints of the crack propagation path and crack closure behavior.

2. Experimental Method

Two types of ferrite-pearlite steels with different pearlite morphologies were prepared as test steels by controlling the TMCP conditions. Steel I is a steel plate comprising ferrite and lamellar pearlite in the plate thickness direction and is classified as a conventional steel. Steel II is the anti-fatigue damage steel plate, AFD™, in which pearlite is uniformly and finely dispersed in the ferrite matrix. The thickness of both samples is 25 mm. The tensile properties of these steel plates are shown in **Table 1**. Small-scale fatigue test specimens of the geometry shown in **Fig. 2** were taken from the test steels. The test specimens of both Steel I and Steel II were taken in such a way that the specimen longitudinal direction was the plate rolling direction and cracks propagated in the plate width direction. This was done in order to investigate the effect of microstructures with different pearlite morphologies, as shown in **Fig. 3**, on the crack propagation direction of the respective specimens. Looking in detail at the distinctive features of the microstructure (pearlite morphology) in the crack propagation direction, Steel I consists of islands of equiaxed ferrite with pearlite existing in a network form surrounding those islands. In contrast, Steel II displays a microstructure in which the pearlite is uniformly and finely dispersed in fine equiaxed ferrite grains. **Table 2** shows the average ferrite grain size and the average pearlite spacing in the crack propagation directions of these respective microstructures.

Table 1 Tensile properties of tested steels

Steel plate	UYS (MPa)	TS (MPa)	El (%)
I	357	486	28.6
II	398	513	22.3

UYS: Upper yield stress TS: Tensile strength El: Elongation

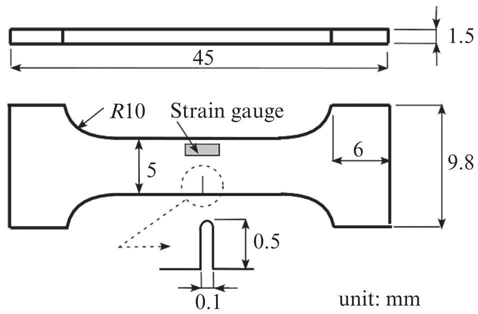

Fig. 2 Geometry of fatigue crack growth specimen

Table 2 Aspects of microstructure

Steel plate	Average ferrite grain size (μm)	Average pearlite spacing (μm)
I	19	62
II	9	26

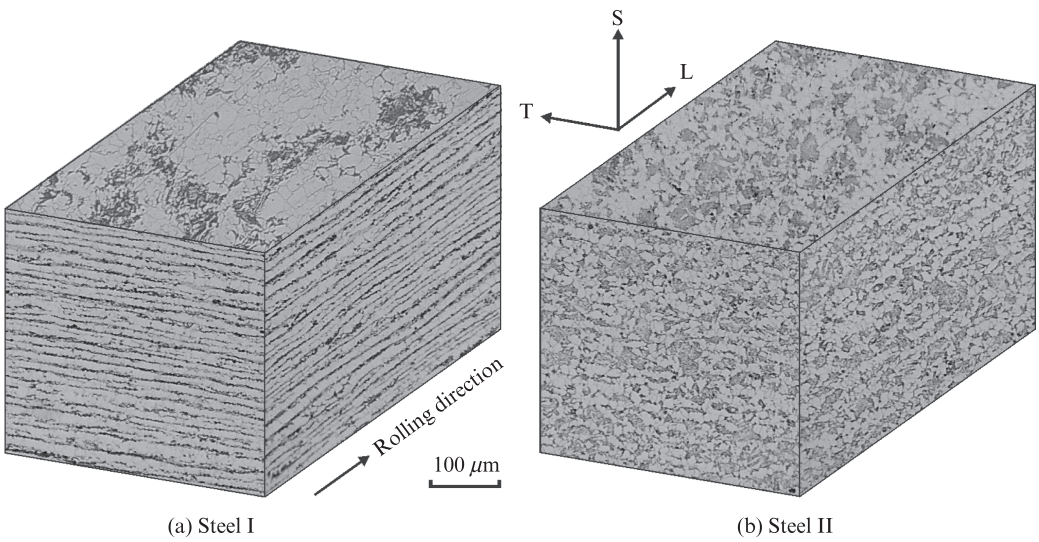

Fig. 3 Microstructures of tested ferritic/pearlitic steels

For detailed observation of the effect of the pearlite morphology on the fatigue crack propagation behavior in the second stage, a fatigue crack propagation test was performed with a constant stress intensity factor range ΔK=15 MPa·m$^{1/2}$, stress ratio R=0.1, and frequency of 2 Hz. This fatigue test was performed in a scanning electron microscope, and the crack growth behavior during the test was observed in detail, at the grain size order, by in-*situ* observation. Crack closure behavior was measured by the unloading elastic compliance method by using a strain gauge attached to the specimen in front of the crack tip, as shown in Fig. 2[6].

3. Experimental Results

3.1 Fatigue Crack Growth Rate and Crack Path

Figure 4 shows the fatigue crack growth rates obtained in the constant ΔK fatigue crack propagation tests. **Figures 5** and **6** show correspondence with the crack growth path, microstructure, and the fatigue crack growth rate for Steel I and Steel II, respectively. These plots of the fatigue crack growth rate were obtained as the average growth rate of the main crack propagating in a length of 50 μm (distance between the white circles shown on the microstructure images in Figs. 5 and 6) projected on the vertical plane relative to the axis of loading. As average values, the fatigue crack growth rate of Steel II, which was 2.1 × 10^{-9} m per cycle, was lower than that of Steel I, which was 5.8 × 10^{-9} m per cycle. Furthermore, in contrast to the fact that Steel II displays

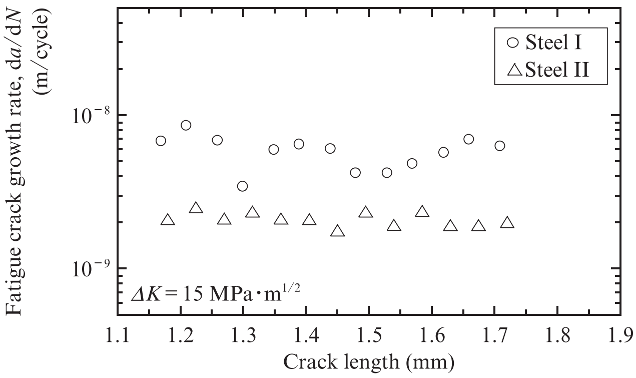

Fig. 4 Fatigue crack growth rates in constant ΔK tests

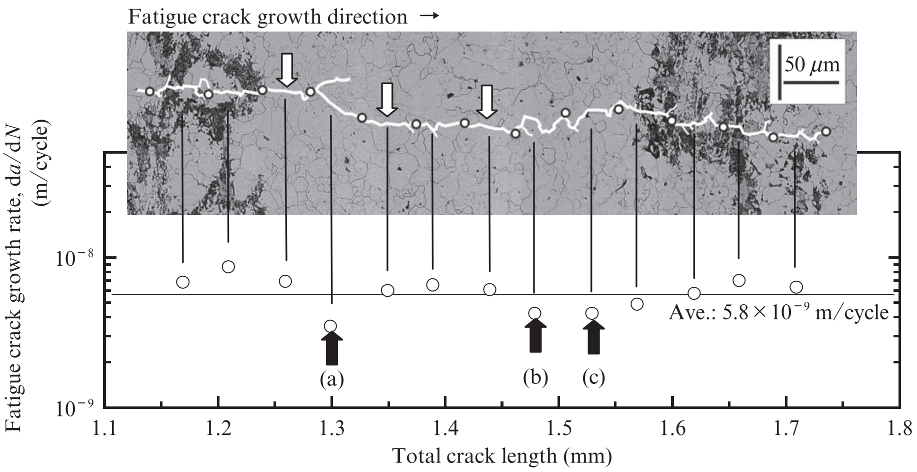

Fig. 5 Fatigue crack growth rate and crack path with microstructure for Steel I

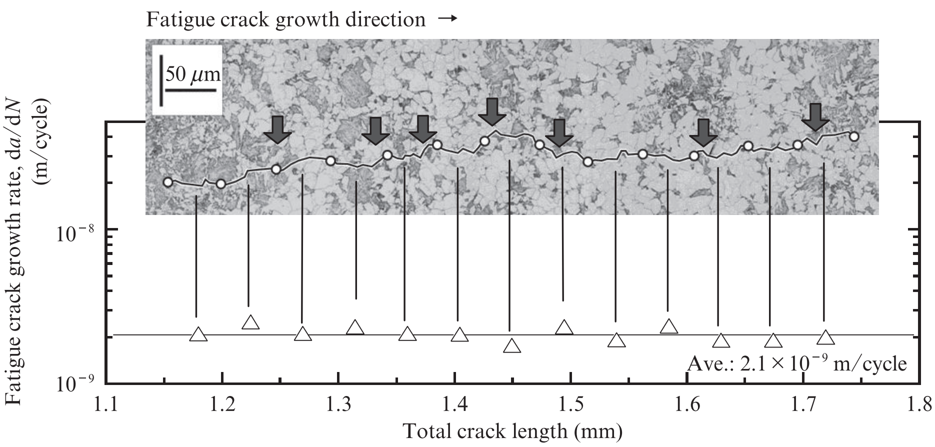

Fig. 6 Fatigue crack growth rates and crack paths with microstructure for Steel II

a stable, low growth rate, the fatigue crack growth rate of Steel I shows considerable variations.

Focusing in greater detail on the relationship between the fatigue crack propagation path and the crack growth rate of Steel I shown in Fig. 5, in the regions where the fatigue crack propagates within ferrite grains, which are shown by the white arrows, propagation is basically linear, and the fatigue crack growth rate at this time is the same or somewhat higher than the average value. In contrast, in parts (a) to (c), which are indicated by the black arrows, crack branching and crack deflection can be observed, and at this time, the fatigue crack growth rate is lower than the average value. Although the fatigue crack growth rate of Steel I displayed large variations, it is suggested that crack deflection and branching play a important role in this phenomenon.

On the other hand, looking at the relationship between the microstructure, crack propagation path, and fatigue crack growth rate of Steel II, which is shown in Fig. 6, it can be understood that finely distributed blocky pearlite exists in the crack propagation path, and the crack deflects in the vicinity of the phase boundary between the ferrite and pearlite phases, as shown by the representative examples indicated by the black arrows in Fig. 6. As mentioned above, crack deflection and branching are thought to induce local decreases in the fatigue crack growth rate. And in Steel II, these deflections occur with high frequency as the crack encounters finely-dispersed pearlite, and it is thought that this behavior is responsible for the stable high fatigue crack growth resistance of Steel II.

3.2 In-*situ* Observation of Fatigue Crack Growth by SEM

The process of deflection of fatigue cracks was investigated in detail by in-*situ* observation using a high magnification scanning electron microscope (SEM). The condition of deflection of the fatigue crack in Steel II, which displayed high fatigue crack growth resistance, is shown in **Fig. 7** in comparison with that of Steel I with low fatigue crack growth resistance. The figure shows the results of in-*situ* observation by SEM, together with schematic illustrations of the corresponding microstructure and the propagation paths (In the photograph of Steel I, pearlite does not exist in the observation plane.). In Steel II, a larger number of deflections of the crack, which are indicated by the red triangles, can be observed in comparison with Steel I, and these crack deflections occur in such a way as to avoid blocky pearlite. This suggests that the pearlite which is finely dispersed in Steel II encourages the phenomenon of deflection of propagating fatigue crack.

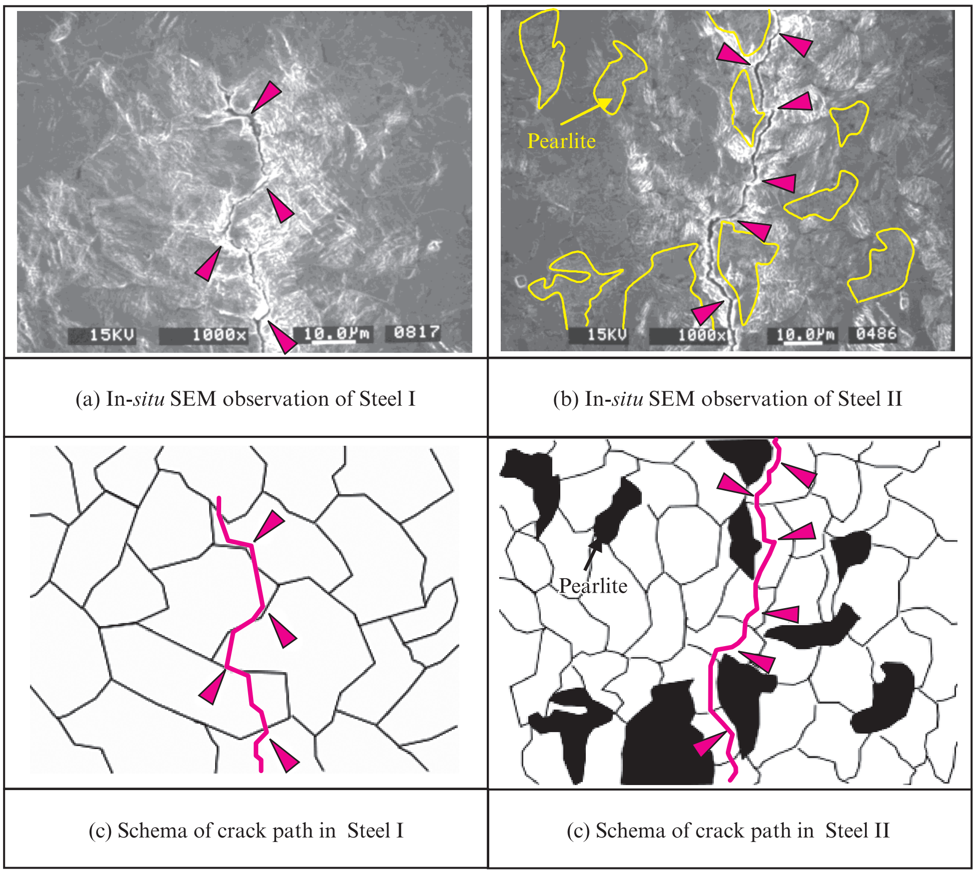

Fig. 7 Crack deflection behavior by in-situ observation

As one interesting point which was obtained by *in-situ* observation of fatigue crack growth within the SEM, the condition of the slip bands in the vicinity of the crack tip differed depending on the test specimen. It is known that the slip bands appear in the plastic region that occurs at the tip of a fatigue crack, and plays a significant role to the crack path.

In Steel I, large slip bands of the fatigue crack tip were developed, as shown by the white striated pattern in the photo in Fig. 7 (a).

On the other hand, in Steel II, the slip bands which occur at the fatigue crack tip are finely dispersed, as show in Fig. 7 (b), and it can be seen that this is the result of blocking of the slip band developments by pearlite, which exists in a blocky form. This slip band morphology is considered to be closely related to crack deflection. That is, it is thought that the constraining force of the ferrite matrix can be enhanced by refinement of the microstructure to a fine ferrite grain size and pearlite spacing, and as a result, fatigue crack deflections occur more frequently and fatigue properties are improved.

4. Discussion

4.1 Improvement of Fatigue Crack Propagation Properties by Crack Closure

The mechanism of fatigue crack growth retardation was studied from the viewpoint of crack closure behavior. **Figure 8** shows the crack opening ratio $U = \Delta K_{eff}/\Delta K$ obtained during fatigue crack growth. Here, ΔK_{eff} is the effective stress intensity factor range considering crack closure. As the value of the crack opening ratio U decreases, the crack closes more easily, expressing the fact that the crack driving force decreases. From this figure, it can be understood that U is lower and crack closure occurs more readily in Steel II than in Steel I. Acceleration of roughness-induced crack closure resulting from the increased frequency of crack deflection is considered to be the main factor in this phenomenon.

Figure 9 shows the relationship between the crack opening ratios and the fatigue crack growth rates of the respective steels. If the driving force of fatigue crack growth depends only on the crack opening ratio, the fatigue crack growth rates of the two steels should be plotted as straight lines having the same slopes. Here, almost all the plots for Steel I fall within a basically straight data band, but the plots related to crack deflection, which were shown by (a) and (b) in Fig. 5, deviate from the data band to the low crack growth rate side. In addition, the fatigue crack growth rate of Steel II, in which fatigue crack deflections were observed with high frequency, clearly is plotted at values of a low crack opening ratio, and the data do not display the expected linear relationship. These results suggest that the fatigue crack growth rate of this material is controlled only by crack closure behavior. Several studies have pointed out that the local crack tip stress intensity factor is reduced by interlocking and branching of cracks[7]. Because it is thought that a different factor, such as a stress shielding effect[7] at the fatigue crack tip, has a large role in retardation of the fatigue crack growth rate, this was studied in the following Section 4.2.

4.2 Stress Shielding Effect at Crack Tip

As shown in Fig. 9, retardation of the fatigue crack growth rate cannot be explained solely by the crack opening ratio. Therefore, a study was carried out in connection with the stress shielding effect at the crack tip, which is known to occur in composite materials such as intermetallic compounds and ceramics. The stress intensity factor at the crack tip K_{tip} is given by Eq. (1)[7].

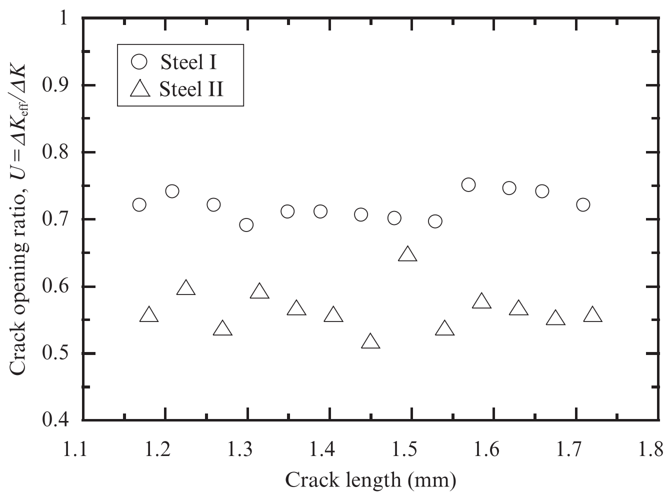

Fig. 8 Crack opening ratio of steels during tests

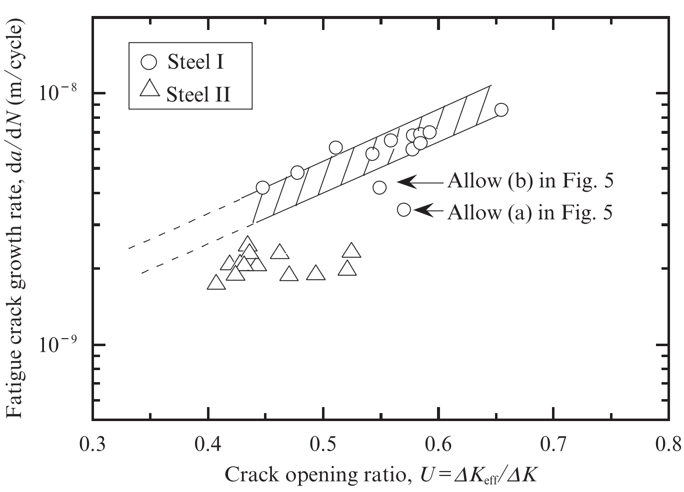

Fig. 9 Comparison between fatigue crack growth rates and crack opening ratio of steels

$$K_{tip}=K_{max}-K_S \quad (1)$$

Here, K_{max} is the stress intensity factor at the maximum stress at which the stress shielding effect does not exist, and K_s is a stress intensity factor related to the stress shielding effect. It is difficult to estimate K_s in complex fatigue crack propagation paths. In the present paper, K_{tip} was calculated by experimentally measuring the crack opening displacement, as shown in **Fig. 10**. From the two equations for the stress intensity factor and crack opening displacement[8)] of a single-edge cracked material having a certain finite width under constant tensile stress, the relationship between K_{tip} and δ_{ideal} can be expressed by Eq. (2).

$$K_{tip}=\frac{\delta_{ideal}E't}{4a}\sqrt{\pi a}\,\frac{F(a/W)}{V(a/W)} \quad (2)$$

Where,

$$F\left(\frac{a}{W}\right)=1.12-0.231\left(\frac{a}{W}\right)+10.55\left(\frac{a}{W}\right)^2-21.72\left(\frac{a}{W}\right)^3+30.39\left(\frac{a}{W}\right)^4,$$

$$V\left(\frac{a}{W}\right)=1.46-0.70\left(\frac{a}{W}\right)+25.93\left(\frac{a}{W}\right)^2-143.0\left(\frac{a}{W}\right)^3+538.6\left(\frac{a}{W}\right)^4-907.5\left(\frac{a}{W}\right)^5+633.7\left(\frac{a}{W}\right)^6$$

E is Young's modulus and v is Poisson's ratio ($E'=E/(1-v^2)$). t is the thickness of the test specimen, a is the crack length, and W is the width of the test specimen. δ_{ideal} is the crack opening displacement of an ideal crack without deflection or branching, as illustrated in Fig. 10 (a).

From Eqs. (1) and (2), at a given crack length a, the crack opening displacement of an ideal crack δ_{ideal}, which has no K_{max} or stress shielding effect, is known to display an linear relationship. Therefore, Eq. (3) is materialized.

$$K_{max}\propto\delta_{ideal} \quad (3)$$

Here, if it is assumed, as a first approximation, that the same relationship exists between K_{tip} and the crack opening displacement δ_{exp} obtained in a fatigue crack propagation experiment including the stress shielding effect, then Eq. (4) is obtained.

$$K_{tip}\propto\delta_{exp} \quad (4)$$

The stress intensity factor of the crack tip can be estimated from Eq. (3) and Eq. (4) by Eq. (5).

$$K_{tip}=\frac{\delta_{exp}}{\delta_{ideal}}K_{max} \quad (5)$$

As shown in **Fig. 11**, the effective stress intensity factor range of a crack tip $\Delta K_{eff,tip}$ can be expressed by Eq. (6).

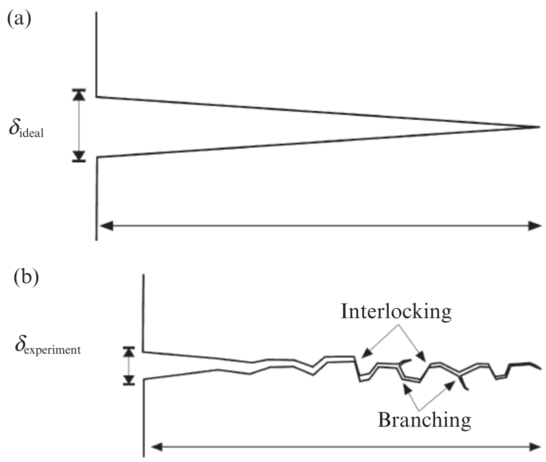

Fig. 10 Crack mouth opening displacement for (a) an ideal crack and (b) a crack with stress shielding effect

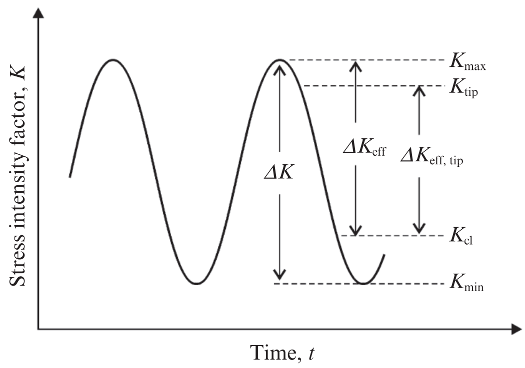

Fig. 11 Schematic determination of the crack tip effective stress intensity factor range

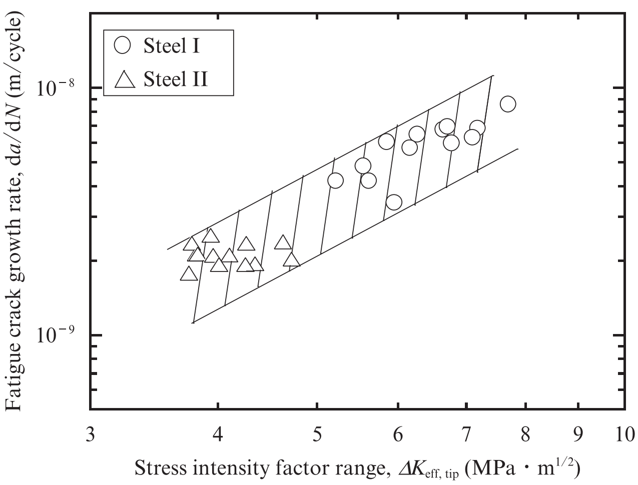

Fig. 12 Relationship between fatigue crack growth rates and $\Delta K_{eff,tip}$

$$\Delta K_{\mathrm{eff,\,tip}} = K_{\mathrm{tip}} - K_{\mathrm{cl}} \quad (6)$$

Here, K_{cl} is the stress intensity factor at the time of crack closure.

Based on the method described above, $\Delta K_{\mathrm{eff,tip}}$ was obtained for Steel I and Steel II, and the relationship with the fatigue crack growth rate was compared. The results are shown in **Fig. 12**. The crack growth rates obtained with two test specimens having different pearlite morphologies can be arranged as one data band by using a single parameter, namely, $\Delta K_{\mathrm{eff,tip}}$, and Steel II, which shows a low fatigue crack growth rate, is positioned in the lower $\Delta K_{\mathrm{eff,tip}}$ region than Steel I. In other words, this study has clarified the fact that, by showing a high frequency of crack deflections, Steel II not only promotes crack closure, but also encourages stress shielding of the crack tip, and as a result, Steel II displays high fatigue crack propagation properties.

5. Conclusion

The fatigue crack propagation behavior of ferrite-pearlite dual-phase steel was investigated in detail by using test steels with different pearlite morphologies, and the mechanism of improvement of fatigue properties was studied. The main conclusions obtained were as follows.

(1) Ferrite-pearlite dual-phase steel with a finely-dispersed pearlite morphology displayed extremely good fatigue properties in the second stage in comparison with a dual-phase steel with a pearlite morphology having a coarse network-like morphology. These improved properties are attributable to frequent deflections of the crack propagation path so as to avoid finely-dispersed blocky pearlite during propagation of a fatigue crack.

(2) In the ferrite-pearlite dual-phase steel with the finely-dispersed pearlite morphology, a higher level of roughness-induced crack closure can be obtained in comparison with the dual-phase steel with a pearlite morphology having a coarse network-like morphology.

(3) The phenomenon of retardation of fatigue crack growth is considered to be due not only to a decrease in ΔK_{eff}, which is attributable to crack closure associated with fatigue crack branching and deflection, but also a decrease in $\Delta K_{\mathrm{eff,tip}}$, which considers stress shielding of the fatigue crack tip through interlocking.

The authors wish to express their appreciation to Prof. Y. Mutoh and Associate Prof. Y. Miyashita of Nagaoka University of Technology for their generous guidance in the fatigue crack propagation experiment and in-*situ* observation of fatigue crack propagation behavior in the SEM and discussion of the mechanism of improvement of fatigue properties in this joint research.

References

1) Miki, C. Science and Technology of Welding and Joining. 2000, vol. 5, no. 6, p. 347.
2) Horn, A. M.; Huther, I.; Lieurade H. P. Welding in the World. 1998, vol. 41, p. 273.
3) Petershagen, H. Welding in the World. 1998, vol. 41, p. 281.
4) Kobayashi, H. Journal of the Society of Materials Science, Japan. 1980, vol. 29, no. 317, p. 198.
5) Igi, S.; Inohara, Y.; Hirai, T. JFE Technical Report. 2005, no. 5, p. 16.
6) Kikukawa, M.; Jono, M.; Tanaka, K.; Takatani, M. Journal of the Society of Materials Science, Japan. 1976, vol. 25, no. 276, p. 899.
7) Mutoh, Y. et al. Materials Science and Engineering A. 2007, vol. 468–470, p. 114.
8) Murakami, Y. Stress Intensity Factors Handbook. Oxford, Peramon Press, 1987, vol. 1, p. 9.